Wall-less Sample Preparation of *μ*m-Sized Sample Spots for Femtomole Detection Limits of Proteins from Liquid Based UV-MALDI Matrices

Michael J. Bogan and George R. Agnes
Department of Chemistry, Simon Fraser University, Burnaby, British Columbia, Canada

Previously, we introduced wall-less sample preparation (WaSP), technology that involves the use of an electrodynamic balance (EDB) to prepare *μ*m-sized sample spots for analysis by matrix-assisted laser desorption/ionization time-of-flight mass spectrometry (MALDI-TOF-MS). In that work we demonstrated the detection of femtomole quantities of a low molecular weight peptide and a hydrophobic ester (both <600 Da). Here we use WaSP to test the hypothesis that the use of small sample spot sizes and an instrument equipped with delayed extraction would increase the analytical utility of liquid sample spots for peptide and protein (>2500 Da) analysis by UV-MALDI-TOF-MS (Sze et al.; J. Am. Soc. Mass Spectrom. **1998,** *9,* 166–174). To aid the optimization of preparing *μ*m-sized sample spots by WaSP, optical microscopy and mass spectrometry were used to investigate nonvolatile solute concentration effects on droplet fission and sample spot size, modifications of the EDB electric field to control droplet ejection, and the use of multiple droplet deposition to increase sample loading. Also described is a rapid deposition mode of operation for WaSP that allows single droplets generated at 1 Hz to be levitated briefly (~500 ms) before being ejected autonomously and deposited as a concentrated sample spot with a spatial accuracy of ±5 *μ*m. To test the sensitivity of the method, one hundred glycerol droplets (270 pL each, 27 nL total) each containing 32 amol lysozyme were deposited on top of each other one-at-a-time to create a single sample spot. Using a mass spectrometer equipped with delayed extraction to analyze this sample spot, we verified the hypothesis of Sze et al. by achieving detection limits three orders of magnitude below that previously observed for the detection of a protein by UV-MALDI-TOF-MS with a chemical-doped liquid matrix sample preparation. (J Am Soc Mass Spectrom 2004, 15, 486–495) © 2004 American Society for Mass Spectrometry

MALDI has helped revolutionize the study of biomolecules by mass spectrometry due, in part, to its ability to create primarily singly charged and intact analyte ions from a sample spot composed of, most commonly, a solid matrix within which the analyte was co-crystallized. Liquid matrices developed for UV-MALDI have been shown to have some useful characteristics, such as increased shot-to-shot reproducibility, but are not commonly used because of adduct formation, relatively poor resolution, and higher detection limits [1–6]. Based on their studies of a chemical-doped glycerol matrix that enabled picomole sensitivities for proteins prepared as a 2 *μ*L sample spot, Sze et al. speculated that the use of smaller matrix droplets and delayed ion extraction could improve the analytical utility of matrix solutions [7]. Here we report the results of experiments designed to test their hypothesis.

The major challenges in attaining sample spots with small diameters (<100 *μ*m) include the manipulation of sub-nanoliter volumes and the spreading of solution upon deposition. Consequently, several researchers have developed dedicated approaches for sample deposition and/or used pre-structured sample supports including the use of piezoelectric droplet deposition [8–10], heated sample plates [11], filling micromachined picoliter vials using a glass micropipette [12], hydrophilic sample anchors on hydrophobic surfaces [13], picoliter syringes [14], and vacuum deposition of a liquid exiting a capillary [15, 16]. All of these techniques result in the formation of solid matrix sample spots and rely on changing the surroundings into or onto which a droplet or liquid stream was deposited, thus requiring some form of pre-structured sample support, heat source, or a sub-atmospheric pressure chamber.

We have previously identified the use of an electrodynamic balance (EDB) coupled with a piezoelectric

Table 1. Composition of solutions loaded into the droplet generator to create droplets that were processed into sample spots using WaSP

| Solution | Analyte | | MALDI matrix | | Solvent composition (% by vol.)* | | | |
	protein or peptide	concentration	chromophore	concentration (mM)	glycerol	H_2O	ACN	TFA
Ia	lysozyme	10 μM	CHCA	9.0	0%	—	—	0.03%
Ib	lysozyme	10 μM	CHCA	9.0	0.8%	—	—	0.03%
Ic	lysozyme	10 μM	CHCA	9.0	3.6%	—	—	0.03%
II	lysozyme	10 μM	sinapinic acid	9.0	0.9%	1%	1%	0.03%
IIIa	lysozyme	120 nM	sinapinic acid	9.0	0.9%	1%	1%	0.03%
IIIb	ACTH (18–39)	200 nM	CHCA	9.0	0.9%	—	—	0.03%
IVa	—	—	—	—	8.0%	—	—	—
IVb	—	—	—	—	2.8%	—	—	—

*all solutions were prepared in spectro grade methanol

droplet generator as an alternative approach for preparing μm-sized sample spots for MALDI-TOF-MS analysis [17]. This approach is different because it modifies the droplet during its transit from the dispenser to the MALDI plate, and in doing so, the aforementioned pre-structured sample supports are not required, though the use of such supports is not precluded. The EDB is a quadrupole ion trap, or Paul trap [18], that uses a combination of DC and AC potentials applied to electrodes to levitate charged liquid droplets of sub-nanoliter volumes at atmospheric pressure [19]. The droplets are typically created from a solution that contains a low volatility component, such as 99:1 methanol and glycerol. While the droplet is trapped in the EDB, rapid evaporative mass transfer of the most volatile component [20], methanol, leaves behind a viscous droplet residue consisting of mainly glycerol and any dissolved solids. This residue is then ejected from the EDB by modifying the electric field and collected on a MALDI plate for offline analysis. Our first application of this technology was focused on the analysis of small molecules (<600 Da). The detection of 1 fmol of leucine enkephalin and 5 fmol of chenodeoxycholic acid diacetate methyl ester in single glycerol droplets that also contained ~420 fmol of an organic MALDI matrix molecule was demonstrated [17]. Therefore, WaSP was a natural fit to test the hypothesis of Sze et al. because it uses glycerol-based droplets to create μm-sized sample spots. After exploring some of the parameters impacting optimal sample spot creation by WaSP, we show that it is capable of increasing the analytical utility of matrix solutions. For example, in consuming <30 nL of starting solution using WaSP, detection limits 3 orders of magnitude lower than that obtained using sample spots created from 2 μL of the same solution were realized for the protein lysozyme.

Experimental

Materials

Glycerol and spectro grade methanol were purchased from BDH (Montreal, Canada). The MALDI matrices

α-cyano-4-hydroxy cinnamic acid (CHCA) and 3,5-dimethoxy cinnamic acid (sinapinic acid), lysozyme, adrenocorticotropic hormone (ACTH) 18-39, trifluoroacetic acid (TFA), and acetonitrile (ACN) were purchased from Sigma (St. Louis, MO). All chemicals were used without further purification. Solutions were prepared in spectro grade methanol as described in Table 1.

Droplet Generation and Levitation

For all studies in this manuscript a piezoelectric droplet-on-demand generator (Uni-photon Systems, model 201, Brooklyn, NY), fitted with an in-house constructed nozzle (40 μm diameter) was used for droplet generation [21]. This device has an internal reservoir of ~3 mL. By contrast, the volume of each droplet produced is on the order of 300 pL and thus the amount of sample wasted is very large. We have since purchased droplet dispensing systems that have an internal reservoir of only 2 μL. At this stage of WaSP development our design objectives were not concerned with the droplet generation step because several commercially available devices exist.

A DC potential applied to an induction electrode positioned 5 mm above the droplet dispenser nozzle imparted an image charge of opposite polarity onto the droplet formed when a voltage pulse was applied to the piezoceramic inside the droplet generator. By setting the induction electrode potential between 0–250 V, the magnitude of the mass-to-charge ratio (m/z) of the droplets levitated in the EDB could be varied. To minimize the disturbance of the trajectories of levitated droplets, the droplet generator, the electrodes of the EDB, and the MALDI plate were enclosed in a plexiglass chamber to eliminate air convection in the laboratory (Figure 1). The EDB consisted of two copper wire (0.9 mm diameter) rings (2 cm diameter) mounted parallel at a separation distance of 6 mm [17]. The amplitude of the 60 Hz AC potential applied to the ring electrodes (AC_{trap}), in phase, ranged from 500 to 2,700 V_{0-P}. The vertical positions of droplets in the EDB were manipulated by the DC potentials applied to the induction electrode and the MALDI plate. Droplets levitated
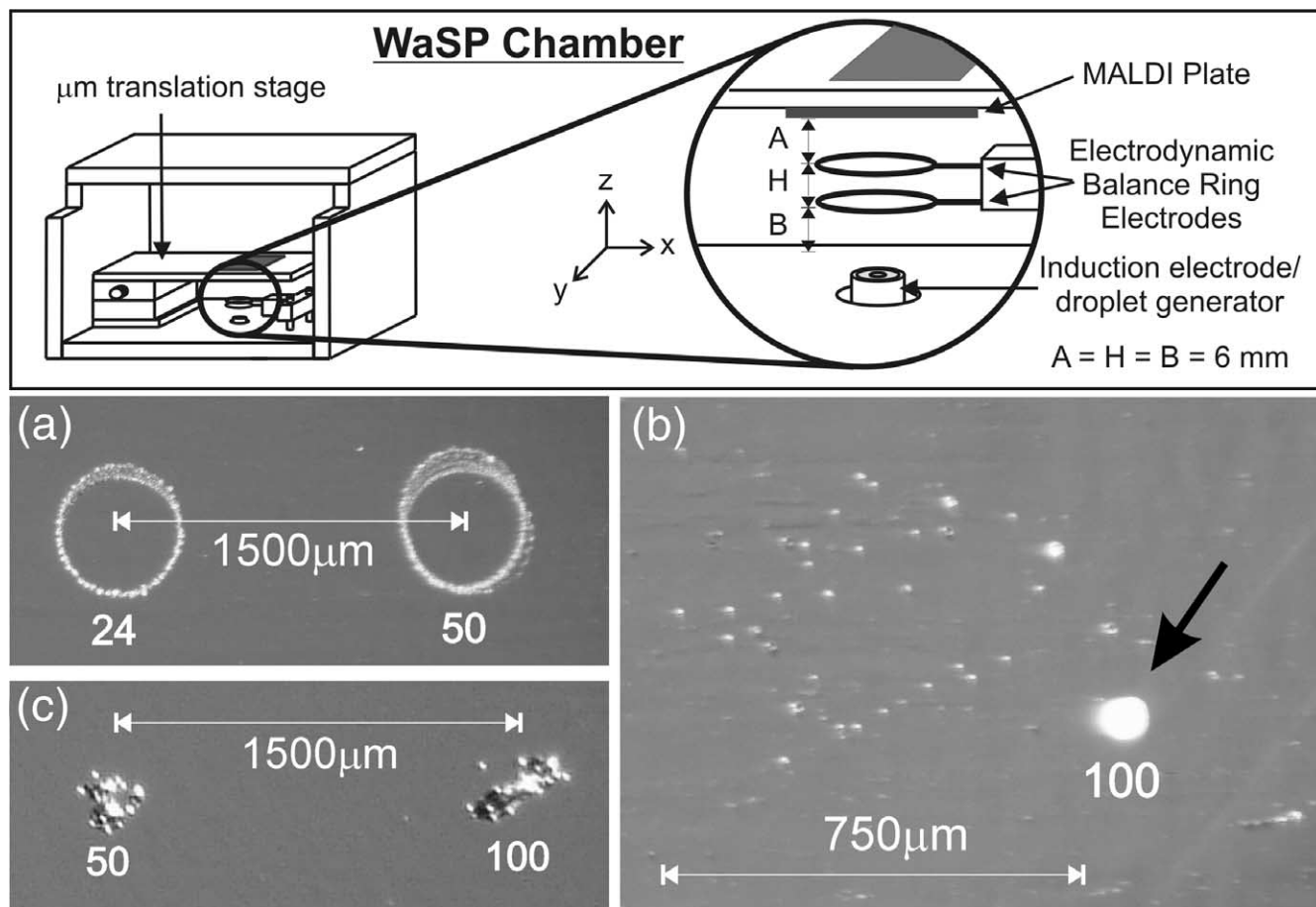
Figure 1. The configuration of the droplet generator, EDB, and MALDI plate that comprise the WaSP apparatus. The sample spots created by depositing, onto a MALDI plate, droplets created from Solution Ia (0% glycerol): (**a**) Droplets that did not pass through an EDB and (**b**) droplets that had been briefly levitated in an EDB. (**c**) The sample spots created by droplets briefly levitated in an EDB created from Solution Ib (0.8% glycerol). The number of droplets deposited at each position is indicated.

in the EDB were illuminated via forward scattering by a 4 mW green HeNe laser (Uniphase model 1676, Manteca, CA). Images of levitated droplets were collected by focusing a digital camera through a microscope objective to the center of the ring electrodes.

Mass Spectrometry

All mass spectra were collected from liquid sample spots (unless otherwise noted) after removing the MALDI plate from the droplet levitation chamber and inserting it into a MALDI-TOF-MS (Perseptive Biosystems Voyager-DE, Framingham, MA). Lysozyme mass spectra were collected with the accelerating voltage = 25 kV, grid voltage = 88.0%, guide wire voltage = 0.030%, delay time = 350 ns, N_2 laser power set at 500 μJ/pulse, and the low mass gate set at 10 kDa. For each sample, the laser was focused at a single position and not moved for the duration of the analysis (the laser spot size has previously been determined to be an oval 190 μm $\times$ 80 μm). The number of laser shots collected is indicated on each mass spectrum. The ACTH 18-39 mass spectrum was the average of 69 laser shots and

that data was collected with the accelerating voltage = 20 kV, grid voltage = 93.7%, guide wire voltage = 0.010%, delay time = 50 ns, N_2 laser power set at 380 μJ/pulse, and the low mass gate set at 800 Da. A mass standard kit (MS-CAL1, Sigma, St. Louis, MO) was used on a daily basis for external mass calibration. Unless otherwise noted, mass spectral data were not smoothed. Signal-to-noise ratios (S/N) were calculated as the peak height divided by one standard deviation of the background signal which was determined using over 300 data points adjacent to the peak of interest. Signal-to-background ratios (S/B) were calculated as the signal divided by the average background signal.

Results and Discussion

The Role of a Surface Tension Modifier on Sample Spot Preparation

Here we illustrate, using both optical (Figure 1) and mass spectral (Figure 2) observations, the advantages and disadvantages of adding a surface tension modifier, such as the low volatility solvent glycerol, to the sample
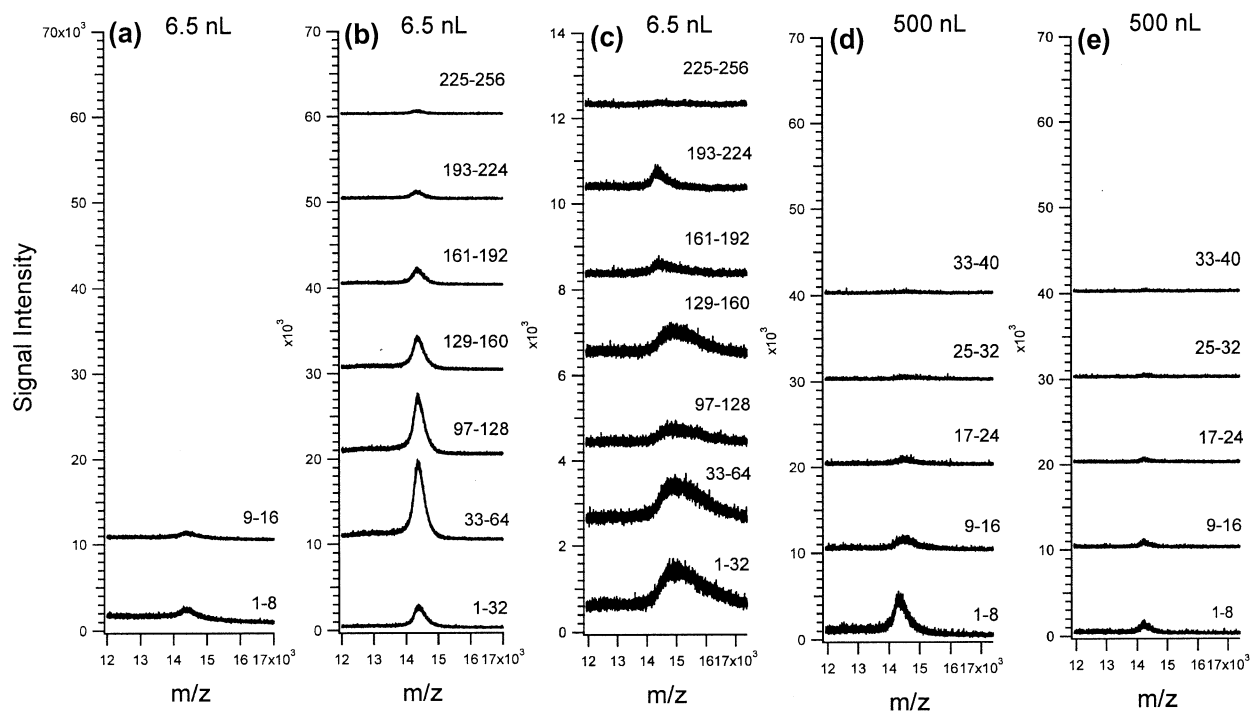
Figure 2. Consecutive mass spectra recorded by firing the laser at the sample spot created by 24 droplets deposited after being levitated in an EDB. The initial droplets were created from Solutions (**a**) Ia (0% glycerol), (**b**) Ib (0.8% glycerol), or (**c**) Ic (3.6% glycerol), all of which contained 10 μM lysozyme. Next, consecutive mass spectra were collected from dried 0.5 μL droplets of Solutions (**d**) Ia and (**e**) Ib, deposited using a 2 μL micropipette. Indicated are the laser shot numbers in the consecutive sequence that were averaged to create the mass spectra displayed and the total volume of sample consumed.

solution when using WaSP to prepare μm-sized sample spots. Solution Ia (Table 1), containing 9 mM CHCA and 10 μM lysozyme, was loaded into the droplet generator and 24 droplets were deposited directly onto the MALDI plate in a single position (co-deposited) without using WaSP. A second spot, positioned 1500 μm from the first, was also created from 50 co-deposited droplets, again without the use of WaSP. Upon impact with the MALDI plate, the liquid from each ~270 pL droplet spread across the surface radially from the impact point, ultimately creating two non-uniform ~520 μm diameter spots of co-crystallized CHCA and lysozyme following the evaporation of the methanol (Figure 1a).

Next, 100 droplets created from Solution Ia were directed through the center of the double ring electrodes (2700 V_{0-P}) of an EDB one-at-a-time and levitated for <500 ms before deposition on the MALDI plate. The majority of the sample material, denoted by a black arrow in Figure 1b, accumulated as a single sample spot of co-crystallized CHCA and lysozyme ~125 μm in diameter. That spot size would suggest a 20 times reduction in area relative to the spot size from the 24 droplets deposited that were not passed through the EDB (Figure 1a). However, Figure 1b also revealed that not all the sample material was deposited in this spot, with some of the material spreading as far as 750 μm

away. The spreading of material observed was due to the evaporating droplets becoming electrostatically unstable during transit through the EDB, causing them to undergo Coulomb fission [22]. In support of these visual observations, the S/N of the lysozyme molecule with a single proton adducted in the mass spectra collected from this spot, denoted by the arrow in Figure 1b, was poor (Figure 2a). Based on knowledge gained from electrospray mass spectrometry analysis of proteins contained in methanol-based charged droplets [23], we speculate that the surface active nature of the lysozyme caused a majority of it to be ejected from the droplet during the fission process. Therefore, when the mass spectra were collected from droplets that had fissioned, a poor signal for lysozyme was obtained because the laser spot size was only 190 μm × 80 μm and much of the protein was outside the laser spot. Note, however, that signals for the matrix were still very prominent (spectra not shown).

To achieve the goal of creating small concentrated sample spots, droplet fission must be eliminated. The amount of net excess charge a droplet can carry is directly proportional to the square root of its surface tension [22], so an increase in the surface tension will reduce the tendency for a droplet to undergo fission. A new solution was made that contained 0.8% glycerol by volume (Solution Ib, Table 1). Collections of 50 and 100

droplets of this solution were deposited, a single drop-let at a time following a brief levitation period in the EDB, at two different positions on the MALDI plate (Figure 1c). Fission was eliminated because a residual levitated droplet consisting almost entirely of glycerol remained after the volatile methanol had evaporated [17]. Having increased each droplet's surface tension, they retained all of their net charge and were deposited within an area ~200 μm in diameter (Figure 1c). The increased analyte density was reflected in the mass spectrum of lysozyme by a 500% increase in the total integrated signal observed (Figure 2b) relative to that prepared without glycerol (Figure 2a). When the per-cent glycerol by volume was increased to 3.6% (Solution Ic, Table 1) the average mass of the lysozyme was shifted to >15 kDa and the resolution decreased (Figure 2c, note y-axis). The integrated peak area was within 7% of that observed for droplets created from Solution Ib, implying that the lysozyme was retained within the glycerol droplets and that the glycerol did not impede ion formation. However, the shift in mass of the ly-sozyme peak was likely due to glycerol adduct forma-tion.

To further investigate the impact of glycerol, two sets of 24 droplets created from Solution Ib were deposited. After insertion of the plate into the vacuum chamber, the first set was analyzed as soon as possible and the second set analyzed after drying under vacuum (~2 × 10^{-7} torr) for 30 min. The resolution for lysozyme from the dried sample (M/Δm = 50, where M = mass of ion and Δm = full width at half maximum) improved by 3.6 times compared with that measured for the sample analyzed immediately (M/Δm = 14). This implied that, due to glycerol evaporation, the composition of the chemical-doped liquid matrix sample spot was chang-ing under vacuum with time and that the effects on desorption plume dynamics by a relatively large amount of glycerol present in the sample spot was likely the source of the poor resolution obtained. These observations are reminiscent of studies of IR-MALDI using glycerol as a matrix where resolution character-istics typically two to three times lower than solid state matrices were observed. There, the poor resolution has been attributed to changes in plume dynamics [24] and thus, in our case, a similar effect may have occurred when the quantity of glycerol present increased.

Glycerol is generally considered to be a contaminant in UV-MALDI. In corroboration, the total integrated signal for lysozyme collected from a single laser posi-tion, centered over a 0.5 μL dried droplet deposited by a 2 μL micropipette from Solution Ib, was only 22% of the signal observed from a 0.5 μL dried droplet pre-pared from Solution Ia (compare Figure 2d, e). How-ever, when comparing the spectra obtained from Solu-tion Ia after preparation by WaSP (6.5 nL consumed, Figure 2b) to the sample prepared by micropipette (500 nL consumed, Figure 2e), a marked increase in S/N and signal longevity was observed. Overall, we have shown that the addition of glycerol to a sample solution being

prepared for MALDI by WaSP is beneficial because it reduces the tendency for droplet fission, thereby con-centrating the sample material before deposition. How-ever, detrimental effects on the mass spectrum such as adduct formation and modification of the desorption properties remain a problem. Nonetheless, the benefits observed from processing a sample solution of interest using WaSP provides impetus for further investigation of the use of WaSP with varied sample deposition characteristics as well as different matrices and ana-lytes.

The Role of Electrode Potentials on Droplet Ejection from an EDB

To further optimize the preparation of μm-sized sample spots by WaSP, we took advantage of the low volatility of glycerol to create droplets that could be levitated in the EDB for long periods of time (hours, if required). All experiments performed in this, and the following sec-tion, used droplets created from a methanol solution containing 8% glycerol (Solution IVa). This enabled us to perform a set of experiments that would optimize droplet trajectory manipulation in, and droplet ejection from, the EDB so that accurate and reproducible droplet deposition could be achieved.

Deposition/balance potential versus AC trapping potential (AC$_{trap}$). A single negatively charged droplet was formed with 75 V applied to the induction electrode [induction potential during droplet formation (IP$_f$)] and the MALDI plate potential held at 0 V. The droplet was trapped in the electric field of the EDB created from AC$_{trap}$ amplitudes set at a fixed value ranging from 700 to 2100 V$_{0-P}$, and then the balance potential (BP) was measured by increasing the DC potential applied to the MALDI plate until the droplet was focused as a single spot in the center of the EDB's two ring electrodes (the null point). Next, the deposition potential (DP), defined as the voltage applied to the MALDI plate necessary to eject the droplet from the EDB and deposit it on the MALDI plate, was determined.

The DP increased as AC$_{trap}$ increased (Figure 3a) because the magnitude of the electric field acting to restore the droplet at the center of the EDB increased. This data concurs with the observation by Wuerker et al. that a particle array can be compressed towards the null point by increasing AC$_{trap}$ [25]. The BP was inde-pendent of AC$_{trap}$ because only the DC potentials were required to offset the force of gravity. Figure 3a displays the data for a single IP$_f$. Droplets produced at IP$_f$ = 25, 50, 100, 125, 150, 175, 200, and 225 V each produced similar trends for BP and DP.

Deposition/balance potential versus induction electrode po-tential (IP). A droplet (IP$_f$ = 100 V) was trapped at AC$_{trap}$ = 960 V$_{0-P}$ and while it was levitated, the potential of the induction electrode was adjusted to a
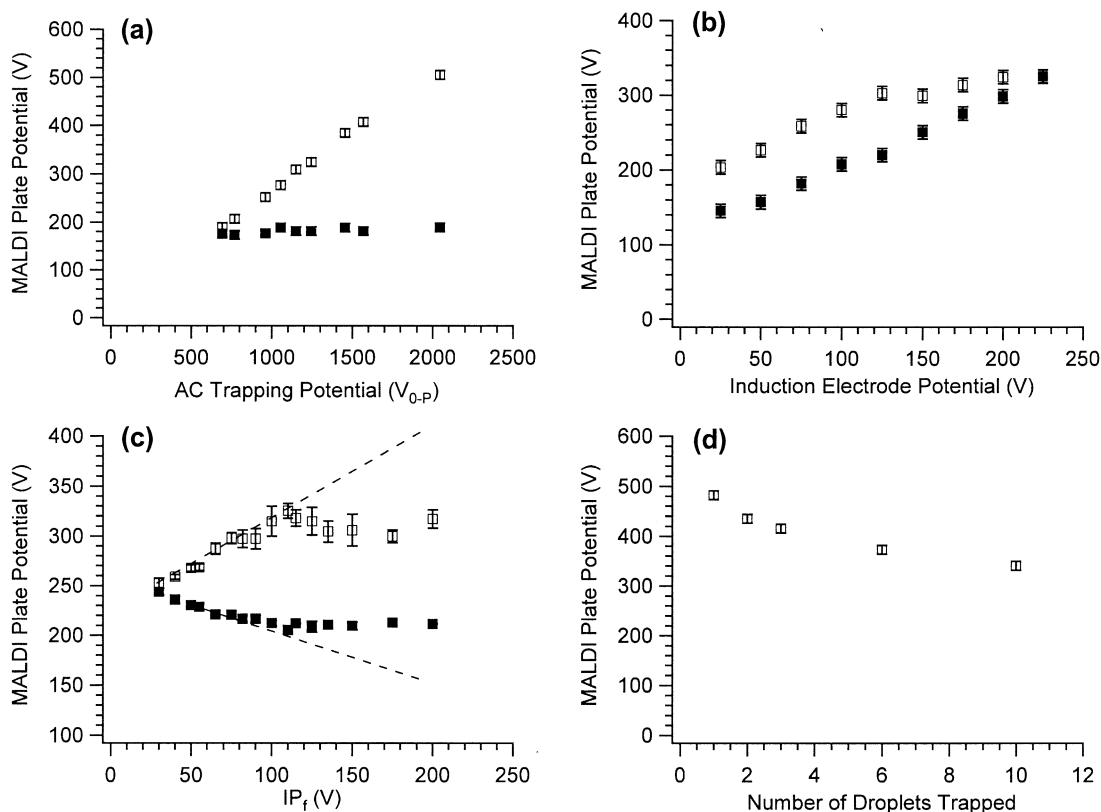
Figure 3. The DC potential applied to the MALDI plate required to balance a single droplet at the null point (BP, filled squares), and eject (DP, open squares) it from the EDB as a function of (**a**) the AC_{trap} with IP_f fixed at 75 V, (**b**) the DC potential applied to the induction electrode with AC_{trap} fixed at 960 V_{0-P} and IP_f fixed at 100 V, and (**c**) the induction potential applied during droplet formation. Lastly, (**d**) the DP of the first droplet from a population of n similarly created droplets levitated in the EDB as a function of n was plotted. All droplets were created from Solution IVa and each data point is the average for seven or more replicates with the error bars representing one standard deviation.

value between 25–200 V (at the same polarity as IP_f). The BP and DP were then measured for the droplet, as described above. For droplets with the same nominal m/z and trapped at the same AC_{trap}, both the DP and BP increased as IP became increasingly positive (Figure 3b). Because the droplet carried net charge of opposite polarity to IP_f it experienced a greater attractive force toward the induction electrode as IP increased. The DP and BP converged at IP > 150 V because the levitated droplet's m/z placed it near the edge of the a-q stability region. Droplets created with IP > 230 V could not be stably levitated at $AC_{trap} = 960\ V_{0-P}$.

Deposition/balance potential versus induction potential during droplet formation (IP$_f$). A single droplet was created with IP_f between 25 and 200 V, and levitated at $AC_{trap} = 1150\ V_{0-P}$. Next, the potential of the induction electrode was set to 100 V and the BP and DP of the droplet were measured. DP increased and BP decreased proportionally with increased IP_f until $IP_f \approx 110$ V (Figure 3c). The dashed lines in Figure 3c are not linear fits of the data and serve only as a guide to emphasize the BP and DP trends. All of the droplets used in this study were created with identical amplitudes applied to the

piezoelectric ceramic in the droplet generator, implying each had the same nominal mass. Therefore, as IP_f increased a larger net charge was induced onto each droplet so the m/z of the droplet decreased. Up until $IP_f \approx 110$ V the droplets with lower m/z (higher mobility) experienced a stronger restoring force at any given fixed AC_{trap}, and thus a deeper trapping potential well depth. Therefore, as IP_f increased, a lower BP was required to balance the droplet, yet a higher DP was required to eject it from the EDB.

Beyond $IP_f = 110$ V, DP, and BP deviated from the previously noted trend because of droplet Coulomb fission. The data for BP and DP when $IP_f > 110$ V was acquired for the largest secondary droplet that remained trapped in the EDB. The erratic behavior in the BP and DP can then be attributed to variability in the amount of charge ejected from the droplets during fission, and possibly the additional factor that the secondary droplet was closer to the edge of the a-q stability region. These results coincided with the observed effects of Coulomb fission on droplet deposition accuracy (Figure 1b) and the associated mass spectra as discussed previously (Figure 2a).
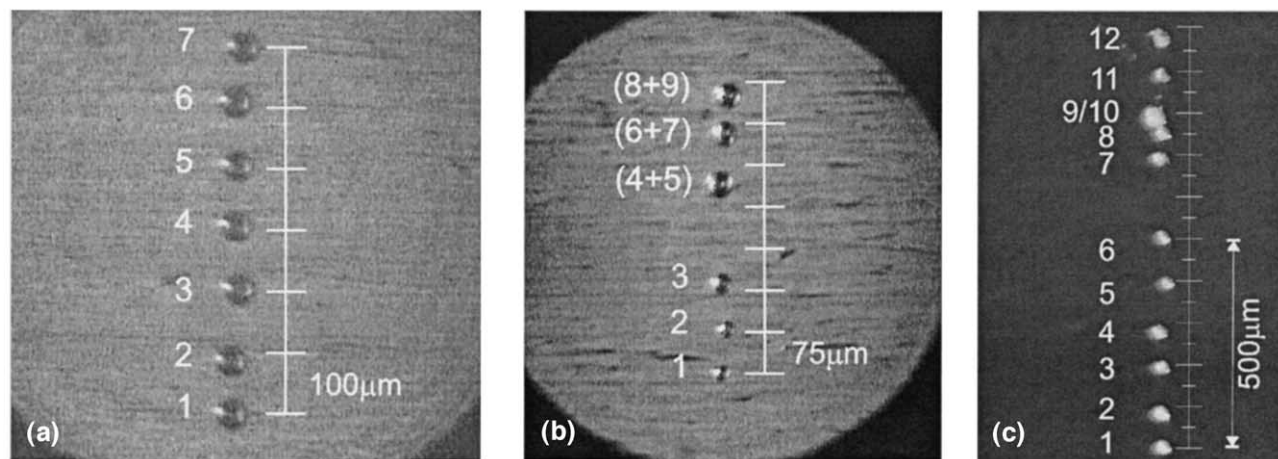
Figure 4. Digital images of arrays of deposited droplets on a MALDI plate prepared from a population of (**a**) 7 droplets created from Solution IVa (8.0% glycerol) and (**b**) 9 droplets created from Solution IVb (2.8% glycerol). (**c**) An array of deposited droplets on a MALDI plate created from Solution Ib (0.8% glycerol) and prepared using rapid deposition of a single droplet at a time (see text). The numbers denote the order of droplet ejection from the EDB, each deposited one at a time.

Deposition potential versus number of droplets trapped. A population of n droplets (n = 1, 2, 3, 6, 10), all created with IP_f = 100 V, were trapped in the EDB. The DP required to eject the first droplet from each population was measured at constant AC_{trap} and was found to decrease as n increased (Figure 3d). The electrostatic repulsion between droplets in the EDB introduces space charge [26]. This perturbation of the trapping potential well depth of the levitated droplets increased in severity as n increased, whereas the relative perturbation with the addition of each droplet to the population decreased as n increased. This can be rationalized by the fact that there is an upper threshold for n, beyond which no more droplets can be added to the population. The largest population able to be levitated was 50 droplets.

Overall, droplet trajectory manipulation was found to be reproducible, with droplets created with low IP_f being the most well-behaved because they were well removed from the Coulomb fission limit. Once droplet manipulation and ejection were well understood, efforts were directed towards characterizing the deposition of droplets onto the MALDI plate.

The Role of Multiple Droplet Co-deposition

Ideally, our goal is to be able to create collections of concentrated sample spots at known positions on a MALDI plate for rapid analysis of the sample without searching for hot spots. To develop this capability we added a translatable MALDI plate to our previously described procedure for ejecting a single droplet at a time from a population levitated in the EDB [17]. In essence, from a population of droplets trapped in the EDB, one droplet at a time was ejected by using an attractive potential applied to the MALDI plate. The position of the MALDI plate relative to the EDB re-

mained stationary or was changed between each droplet ejection event, thereby enabling multiple droplet co-deposition or the creation of an array of deposited droplets, respectively.

Figure 4a is a picture of an array of deposited droplets 50 μm in diameter created from Solution IVa. When the center-to-center (c-c) spacing was decreased to <100 μm, the propensity for two adjacent droplets to coalesce increased. Next, an array was formed from nine droplets created from a starting solution (Solution IVb) that contained 2.8% glycerol in methanol (Figure 4b). Droplets 1–3 were deposited individually at a c-c separation distance of 75 μm and had a deposited diameter of 17 μm. Droplets 4–9 were deposited as two droplets per deposition position, at 75 μm spacing, beginning 150 μm from Droplet 3. This created the three larger sample spot sizes (50 μm diameter) in the upper half of Figure 4b. This demonstrated the flexibility in both the number of droplets deposited at any one position and the spacing between the site of deposition available with this technology, as well as the ability to create higher density arrays by using a lower concentration of glycerol to create smaller droplets.

In forming arrays of droplets using WaSP, once levitated, the population of droplets can be trapped for a delay time ranging from seconds to hours in length before they are deposited, depending on the evaporation rate of solvents from the levitated droplets and the mass of nonvolatile material present. For methanol, we found that this time can be reduced to ~500 ms. Single droplets were created (IP_f = 20 V) at a frequency of 1 Hz while AC_{trap} = 2700 V with the potential applied to the MALDI plate set at 200 V. This caused each droplet to be briefly trapped in the EDB, allowing the methanol to evaporate. In <1 s each droplet escaped the electric field of the EDB and was ejected along the z axis at x = y = 0. By moving the MALDI plate between each droplet
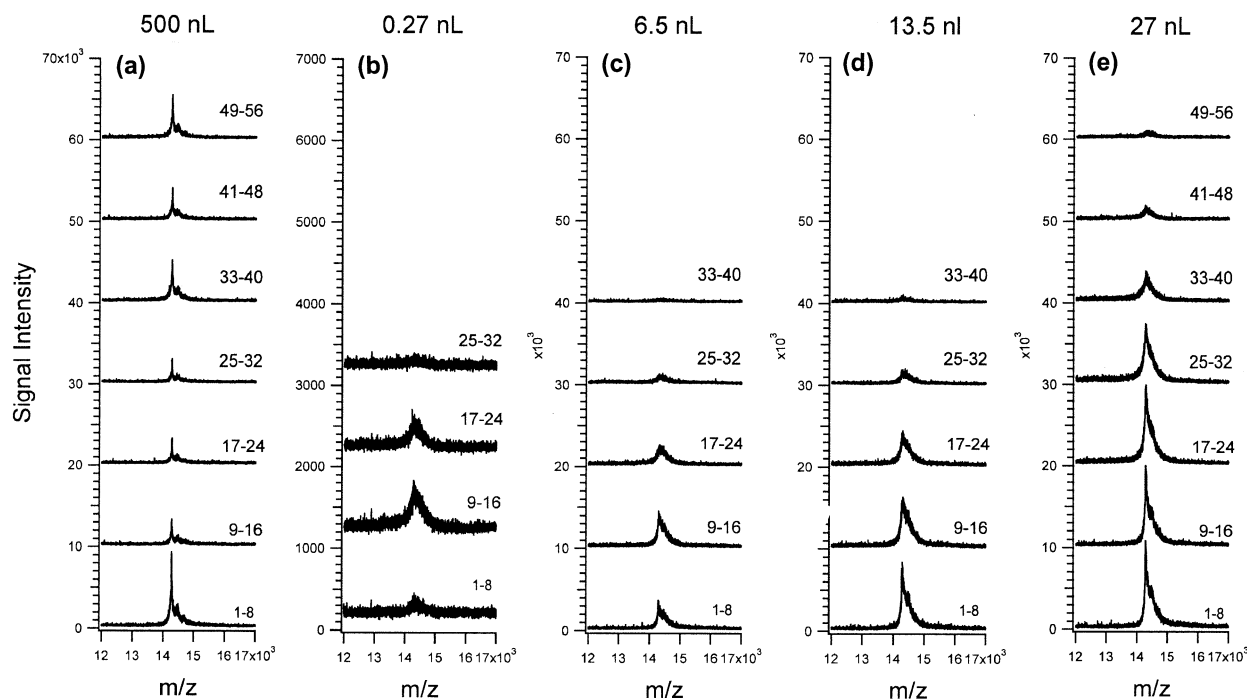
Figure 5. Consecutive mass spectra collected from Solution II, containing 10 μM lysozyme and 0.9% glycerol, prepared as a (**a**) 0.5 μL dried droplet delivered by a 2 μL micropipette or as (**b**) 1, (**c**) 24, (**d**) 50, or (**e**) 100 droplets by WaSP. Indicated are the laser shot numbers in the consecutive sequence that were averaged to create the mass spectra displayed and the total volume of sample consumed.

generation event, an array of deposited droplets was formed. For example, using Solution II (10 μM lysozyme and 0.9% glycerol), six droplets were deposited at intervals of 100 μm (Figure 4c). The MALDI plate was moved 200 μm after the sixth droplet had been deposited, and then another six droplets were deposited at intervals of 50 μm. All of the droplets spaced with 100 μm intervals were deposited without coalescence whereas two of the droplets from the more closely spaced array coalesced, suggesting that 50 μm was near the lower limit of the c-c spacing capabilities of this technique under these conditions. The accuracy of droplet deposition using both the rapid deposition and single droplet deposition from a population, was measured by comparing the final position of the deposited droplets with their expected positions, yielding an average variation of ± 5 μm. A major source of this variation may have been the manual micrometer translation of the MALDI plate. Work is ongoing to improve the accuracy and flexibility of this procedure by introducing computer control over the MALDI plate translation and the potentials applied to the EDB electrodes, all synchronized to the droplet generation event.

Using the array making capabilities described above, we investigated the impact of sample loading on mass spectra. Collections of droplets (1, 24, 50, and 100) prepared by rapid deposition from a methanol solution containing 10 μM lysozyme and 0.9% glycerol (Solution II) were analyzed and compared to a sample of the same solution prepared as a 0.5 μL dried droplet

(Figure 5). Using the same laser power setting, the ion signals detected from consecutive sets of eight laser shots were averaged to produce the mass spectra shown. As the number of droplets deposited was increased from 1 to 100 the S/N for lyzozyme in the spectrum created from the average of the first eight laser shots increased from 25 to 169 and the signal-to-background ratio (S/B) increased from 3 to 36, respectively. Furthermore, after 40 laser shots had been fired at the 24 droplet sample the S/N = 2 and the S/B = 9 whereas for the 100 droplet sample, even after 56 laser shots the S/N = 4 and S/B = 18, reflecting a marked gain in the longevity of the signal with increased sample loading. In conjunction, the total integrated signal increased by a factor of 25 when comparing the single droplet versus the 100 droplets.

It is important to note that if the laser was moved or a higher power setting (leading to a larger laser spot size) was applied to the laser after the collection of mass spectra in Figure 5, high lysozyme signal intensities were re-established for the 24–100 droplet samples. For example, with a collection of 100 droplets of Solution II, 3200 laser shots could be fired in total before the entire sample was consumed. This implied that the non-linear increase in total integrated signal with number of droplets deposited was because all of the droplets were not irradiated within the spot size of the focused laser. Nonetheless, multiple droplet co-deposition was found to be effective in improving detection capabilities and therefore this approach will be used when attempting to
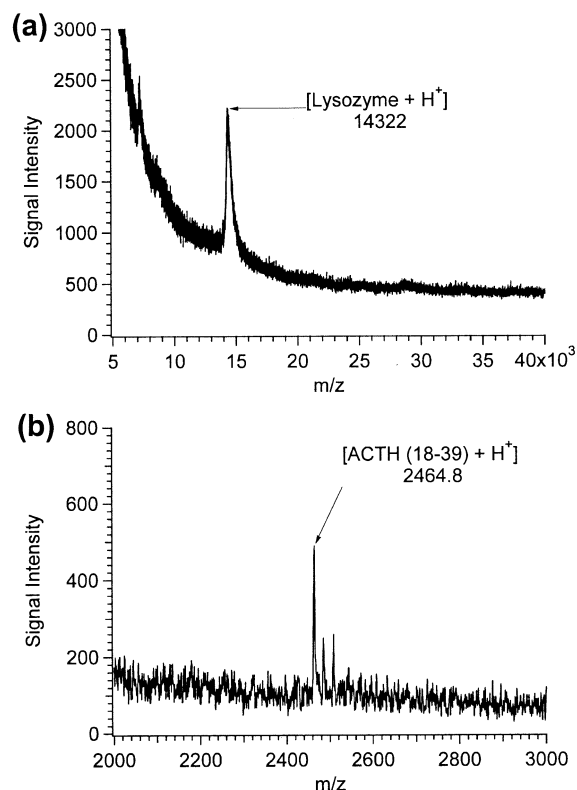
Figure 6. The mass spectra collected from (**a**) 100 WaSP co-deposited droplets of Solution IIIa each containing 32 amol lysozyme (total volume consumed = 27 nL, total analyte deposited = 3.2 fmol) and (**b**) 46 WaSP co-deposited droplets of Solution IIIb, each containing 53 amol ACTH (18-39) (total volume consumed = 12 nL, total analyte deposited = 5.3 fmol). Both mass spectra were smoothed with a boxcar average of 5 points.

characterize samples that have low analyte concentration.

*Detection of fmol Quantities of a Peptide
or Protein from μm-Sized Liquid Sample Spots*

At its present state the combined capabilities of WaSP to preconcentrate and increase sample loading have enabled the detection of lysozyme (S/N = 98, resolution = 26) in a 120 nM starting solution (Solution IIIa) when 100 droplets were co-deposited (Figure 6a). Assuming 40 μm radius (270 pL) droplets initially, the 32 amol of lysozyme in each levitated droplet was concentrated by a factor of ~120 after each had shrunk to ~2.2 pL. In addition, by depositing 100 droplets onto the plate in the same spot, the sample loading was increased by 100 times to a total of 3.2 fmol deposited. However, recall that the sample spot created from the 100 droplets was larger than the laser spot diameter. So, if the laser remained stationary, the entire sample was not irradiated and not all of the 3.2 fmol was available for detection. WaSP was also used to detect ACTH 18-39 (S/N = 35, resolution = 500) from 46 co-deposited droplets of a 200 nM solution (Solution IIIb), corre-

sponding to 53 amol per droplet and a total of 5.3 fmol deposited (Figure 6b). The relative low resolution as well as the presence of sodium and potassium adducts imply that there is still room for improvement in the WaSP detection of peptides.

The matrices used were classified as chemical-doped liquid matrices by Sze et al. when they developed a CHCA-doped glycerol matrix that enabled picomole sensitivities for proteins from a 2 μL sample spot [7]. In their conclusion they hypothesized that lower detection limits could be attained using smaller sample spots and delayed extraction. By using WaSP to deposit one hundred 270 pL droplets and using a mass spectrometer equipped with delayed extraction, we have verified their hypotheses by demonstrating detection limits three orders of magnitude below that previously observed for the detection of a protein by UV-MALDI-TOF-MS with a CHCA-doped liquid matrix sample preparation while consuming only 27 nL of sample.

For comparison, another example of a chemical-doped liquid matrix developed by Williams and Fenselau, *p*-nitroaniline/glycerol, was found to be better suited for sugars and oligonucleotides than peptides, as supported by detection limits of 800 fmol for the conserved N-linked oligosaccharide trimannosyl core, 56 fmol for the oligonucleotide hexamer GAATTC, and 5 pmol for insulin [5]. A positive-ion MALDI spectrum of 95 pmol of carbonic anhydrase with a resolution similar to that obtained with sinapinic acid and 2,5 dihydroxybenzoic acid was also reported. However, it was mentioned that adduct formation occurred with holo-metallothionein, hen egg white lysozyme, and cytochrome *c* which consequently decreased resolution. Although no mass spectra displaying this effect were included, we suspect that the adduction was similar to what we have observed here and thus was likely also due to glycerol. In contrast, they reported that the sugars and oligonucleotides did not experience this adduction problem so analyses of those classes of compounds are another potential application of WaSP using chemical-doped liquid matrices.

In terms of the analysis of lysozyme in samples prepared by WaSP, similar adduct formation problems lead to less resolved signals, and decreased longevity of a lysozyme signal relative to that obtainable from the same solution deposited as a 0.5 μl droplet using a 2 μL micropipette (Figure 5a and c) when sinapinic acid was used as the matrix. However, for samples prepared in the same manner but using CHCA as the matrix we observed better resolution and signal longevity for WaSP sample spots (compare Figure 2b and e). These conflicting results reveal that there are complex issues yet to be resolved in the application of WaSP to the UV-MALDI of samples containing proteins, perhaps leading to unforeseen benefits in the future. We speculate that improvements in mass spectral resolutions and reduced detection limits may be obtained with WaSP by making optimal modifications and/or substitutions in droplet composition and matrix choice that circumvent

droplet Coulomb fission while avoiding adverse effects on UV-MALDI MS performance. Approaches being investigated include modifications of this chemical-doped liquid matrix system or the use of an entirely different one, such as a chemical liquid matrix. The most intriguing set of candidates at this point is the suite of ionic liquid matrices for MALDI that were recently introduced [27]. Alternatively, glycerol is commonly used as a matrix for IR-MALDI [24], suggesting another avenue of future application for μm-sized glycerol containing sample spots created by WaSP.

Conclusion

Several key chemical and instrumental parameters governing the creation of μm-sized droplets using WaSP have been described in detail. Droplet delivery at 1 Hz by WaSP was used to create sample spots of high analyte density by co-depositing up to 100 droplets in a region whose size was on the same order as the spot size of the laser output used to analyze them. Such μm-sized sample spots were then shown to increase the analytical utility of liquid-based MALDI matrices, resulting in drastically reduced detection limits of peptides and proteins while consuming <30 nanoliters of sample. Overall, the features of WaSP investigated here and the new developments described emphasize the versatility of the technology for the preparation of sample spots for UV-MALDI-TOF-MS, and further investigations of its use with other liquid matrix systems, IR lasers, and its potential as a preconcentration device prior to offline MALDI-TOF-MS were suggested.

Acknowledgments

References

1. Zhao, S.; Somayajula, K. V.; Sharkey, A. G.; Hercules, D. M.; Hillenkamp, F.; Karas, M.; Ingendoh, A. *Anal. Chem.* **1991,** *63,* 450–453.
2. Chan, T.-W.; Colburn, A. W.; Derrick, P. J. *Org. Mass Spectrom.* **1992,** *27,* 53–56.
3. Cornett, D. S.; Duncan, M. A.; Amster, I. J. *Anal. Chem.* **1993,** *65,* 2608–2613.
4. Zollner, P.; Stubiger, G.; Schmid, E.; Pittenauer, E.; Allmaier, G. *Int. J. Mass Spectrom.* **1997,** *69/170,* 99–109.
5. Williams, T. L.; Fenselau, C. *Eur. Mass Spectrom.* **1998,** *4,* 379–383.
6. Ring, S.; Rudich, Y. *Rapid Commun. Mass Spectrom.* **2000,** *14,* 515–519.
7. Sze, E. T. P.; Chan, T.-W. D.; Wang, G. *J. Am. Soc. Mass Spectrom.* **1997,** *9,* 166–174.
8. Yogi, O.; Kwawkami, T.; Yamauchi, M.; Ye, J. Y.; Ishikawa, M. *Anal. Chem.* **2001,** *73,* 1896–1902.
9. Johnson, T.; Bergquist, J.; Ekman, R.; Nordhoff, E.; Schürenberg, M.; Klöppel, K.-D.; Müller, M.; Lehrach, H.; Gobom, J. *Anal. Chem.* **2001,** *73,* 1670–1675.
10. Little, D. P.; Cornish, T. J.; O'Donnel, M. J.; Braun, A.; Cotter, R. J.; Koster, H. *Anal. Chem.* **1997,** *69,* 4540–4546.
11. Onnerfjord, P.; Nilsson, J.; Wallman, L.; Laurell, T.; Marko-Varga, G. *Anal. Chem.* **1998,** *70,* 4755–4760.
12. Jespersen, S. *Rapid Commun. Mass Spectrom.* **1994,** *8,* 581–584.
13. Schuerenberg, M.; Luebbert, C.; Eickhoff, H.; Kalkum, M.; Lehrach, H.; Nordhoff, E. *Anal. Chem.* **2000,** *72,* 3436–3442.
14. Keller, B. O.; Li, L. *J. Am. Soc. Mass Spectrom.* **2001,** *12,* 1055–1063.
15. Preisler, J.; Hu, P.; Rejtar, T.; Moskovets, E.; Karger, B. L. *Anal. Chem.* **2002,** *74,* 17–25.
16. Retjar, T.; Hu, P.; Juhasz, P.; Campbell, J. M.; Vestal, M. L.; Preisler, J.; Karger, B. L. *J. Proteome Res.* **2002,** *1,* 171–179.
17. Bogan, M. J.; Agnes, G. R. *Anal. Chem.* **2002,** *74,* 489–496.
18. Paul, W. *Rev. Modern Phys.* **1990,** *62,* 531–540.
19. Davis, E. J. *Aerosol Sci. Technol.* **1997,** *26,* 212–254.
20. Zhu, J.; Zheng, F.; Laucks, M. L.; Davis, E. J. *J. Colloid Int. Sci.* **2002,** *249,* 351–358.
21. Feng, X.; Agnes, G. R. *J. Am. Soc. Mass Spectrom.* **2000,** *11,* 393–399.
22. Taflin, D. C.; Ward, T. L.; Davis, E. J. *Langmuir* **1989,** *5,* 376–384.
23. Fenn, J. B.; Mann, M.; Meng, C. K.; Wong, S. F.; Whitehouse, C. M. *Mass Spectrom. Rev.* **1990,** *9,* 37–70.
24. Dreisewerd, K.; Berkenkamp, S.; Leisner, A.; Rohlfing, A.; Menzel, C. *Int. J. Mass Spectrom.* **2003,** *226,* 189–209.
25. Wuerker, R. F.; Shelton, H.; Langmuir, R. V. *J. Appl. Phys.* **1959,** *30,* 342.
26. Vehring, R.; Aardahl, C. L.; Davis, E. J.; Schweiger, G.; Covert, D. S. *Rev. Sci. Instrum.* **1997,** *68,* 70–78.
27. Armstrong, D. W.; Zhang, L.; He, L.; Gross, M. L. *Anal. Chem.* **2001,** *73,* 3679–3686.